Report No. CG-D-22-95

# PROBABILITY OF DETECTION AND CLASSIFICATION USING USCG SURVEILLANCE

***Annex C of Cost and Operational Effectiveness Analysis for Selected International Ice Patrol Mission Alternatives***

DTIC
ELECTE
OCT 2 6 1995
S D
F

Robert L. Armacost

EER Systems Corporation
Vienna, VA

FINAL REPORT

JUNE 1995

DISTRIBUTION STATEMENT A
Approved for public release
Distribution Unlimited

This document is available to the U.S. public through the
National Technical Information Service, Springfield, Virginia 22161

Prepared for:

19951024 166

U.S. Coast Guard
Research and Development Center
1082 Shennecossett Road
Groton, Connecticut 06340-6096

and

DTIC QUALITY INSPECTED 5

U.S. Department Of Transportation
United States Coast Guard
Office of Engineering, Logistics, and Development
Washington, DC 20593-0001

# NOTICE

This document is disseminated under the sponsorship of the Department of Transportation in the interest of information exchange. The United States Government assumes no liability for its contents or use thereof.

The United States Government does not endorse products or manufacturers. Trade or manufacturers' names appear herein solely because they are considered essential to the object of this report.

The contents of this report reflect the views of the Coast Guard Research & Development Center. This report does not constitute a standard, specification, or regulation.


G. T. Gunther
Technical Director, Acting
United States Coast Guard
Research & Development Center
1082 Shennecossett Road
Groton, CT 06340-6096

Technical Report Documentation Page

| 1. Report No. CG-D-22-95 | 2. Government Accession No. | 3. Recipient's Catalog No. |
|---|---|---|

4. Title and Subtitle

PROBABILITY OF DETECTION AND CLASSIFICATION USING USCG SURVEILLANCE
Cost and Operational Effectiveness Analysis for Selected International Ice Patrol Mission Alternatives, Annex C

5. Report Date
March, 1995

6. Performing Organization Code

8. Performing Organization Report No.
R&DC 21/95

7. Author(s)
Armacost, Robert L.

9. Performing Organization Name and Address

EER Systems Corporation
1593 Spring Hill Road
Vienna, VA 22182

10. Work Unit No. (TRAIS)

11. Contract or Grant No.
DTCG39-94-C-E00085

13. Type of Report and Period Covered
Final Report
July, 1994 to June, 1995

12. Sponsoring Agency Name and Address

U.S. Department of Transportation
U.S. Coast Guard
Office of Engineering, Logistics, and Development
Washington, DC 20593-0001

United States Coast Guard
Research and Development Center
1082 Shennecossett Road
Groton, CT 06340-6069

14. Sponsoring Agency Code

15. Supplementary Notes

16. Abstract

This report is Interim Report Volume 3 for the Cost and Operational Effectiveness Analysis for Ice Patrol Mission Analysis Study. This report examines the probability of detection and classification using USCG surveillance. The various studies of the performance of the AN/APS-135 SLAR system have provided empirical data on which estimates of the probability of detection of various ice targets can be based. Using those results, estimates of the probability of detection, adjusted for operator misinterpretations and misclassifications, were computed and used in a model to estimate search effectiveness and system effectiveness for ice target types. The available study on the AN/APS-137 FLAR system was insufficient to permit a comparable analysis. However, rough estimates of overall FLAR search and system effectiveness were computed. Both the system effectiveness and the search effectiveness for the FLAR system were less than that for the SLAR system.

17. Key Words

International Ice Patrol
Icebergs
Surveillance

18. Distribution Statement

Document is available to the U.S. public through the National Technical Information Service
Springfield, VA 22161

| 19. Security Classif. (of this report) | 20. SECURITY CLASSIF. (of this page) | 21. No. of Pages | 22. Price |
|---|---|---|---|
| Unclassified | Unclassified | 25 | |

Form DOT F 1700.7 (8/72)

Reproduction of form and completed page is authorized

# METRIC CONVERSION FACTORS

## Approximate Conversions to Metric Measures

| Symbol | When You Know | Multiply By | To Find | Symbol |
|---|---|---|---|---|
| | **LENGTH** | | | |
| in | inches | * 2.5 | centimeters | cm |
| ft | feet | 30 | centimeters | cm |
| yd | yards | 0.9 | meters | m |
| mi | miles | 1.6 | kilometers | km |
| | **AREA** | | | |
| $in^2$ | square inches | 6.5 | square centimeters | $cm^2$ |
| $ft^2$ | square feet | 0.09 | square meters | $m^2$ |
| $yd^2$ | square yards | 0.8 | square meters | $m^2$ |
| $mi^2$ | square miles | 2.6 | square kilometers | $km^2$ |
| | acres | 0.4 | hectares | ha |
| | **MASS (WEIGHT)** | | | |
| oz | ounces | 28 | grams | g |
| lb | pounds | 0.45 | kilograms | kg |
| | short tons (2000 lb) | 0.9 | tonnes | t |
| | **VOLUME** | | | |
| tsp | teaspoons | 5 | milliliters | ml |
| tbsp | tablespoons | 15 | milliliters | ml |
| fl oz | fluid ounces | 30 | milliliters | ml |
| c | cups | 0.24 | liters | l |
| pt | pints | 0.47 | liters | l |
| qt | quarts | 0.95 | liters | l |
| gal | gallons | 3.8 | liters | l |
| $ft^3$ | cubic feet | 0.03 | cubic meters | $m^3$ |
| $yd^3$ | cubic yards | 0.76 | cubic meters | $m^3$ |
| | **TEMPERATURE (EXACT)** | | | |
| °F | Fahrenheit temperature | 5/9 (after subtracting 32) | Celsius temperature | °C |

*1 in = 2.54 (exactly).

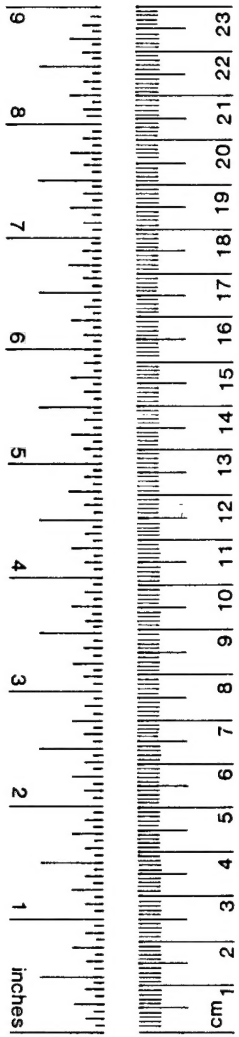


## Approximate Conversions from Metric Measures

| Symbol | When You Know | Multiply By | To Find | Symbol |
|---|---|---|---|---|
| | **LENGTH** | | | |
| mm | millimeters | 0.04 | inches | in |
| cm | centimeters | 0.4 | inches | in |
| m | meters | 3.3 | feet | ft |
| m | meters | 1.1 | yards | yd |
| km | kilometers | 0.6 | miles | mi |
| | **AREA** | | | |
| $cm^2$ | square centimeters | 0.16 | square inches | $in^2$ |
| $m^2$ | square meters | 1.2 | square yards | $yd^2$ |
| $km^2$ | square kilometers | 0.4 | square miles | $mi^2$ |
| ha | hectares (10,000 $m^2$) | 2.5 | acres | |
| | **MASS (WEIGHT)** | | | |
| g | grams | 0.035 | ounces | oz |
| kg | kilograms | 2.2 | pounds | lb |
| t | tonnes (1000 kg) | 1.1 | short tons | |
| | **VOLUME** | | | |
| ml | milliliters | 0.03 | fluid ounces | fl oz |
| l | liters | 0.125 | cups | c |
| l | liters | 2.1 | pints | pt |
| l | liters | 1.06 | quarts | qt |
| l | liters | 0.26 | gallons | gal |
| $m^3$ | cubic meters | 35 | cubic feet | $ft^3$ |
| $m^3$ | cubic meters | 1.3 | cubic yards | $yd^3$ |
| | **TEMPERATURE (EXACT)** | | | |
| °C | Celsius temperature | 9/5 (then add 32) | Fahrenheit temperature | °F |

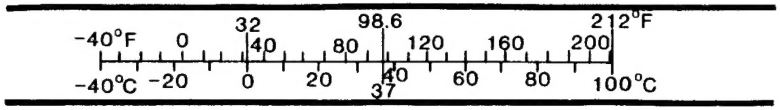

# PROBABILITY OF DETECTION AND CLASSIFICATION USING USCG SURVEILLANCE


## ABSTRACT

The various studies of the performance of the AN/APS-135 SLAR system have provided empirical data on which estimates of the probability of detection of various ice targets can be based. Using those results, estimates of the probability of detection, adjusted for operator misinterpretations and misclassifications, were computed and used in a model to estimate search effectiveness and system effectiveness for ice target types. The available study on the AN/APS-137 FLAR system was insufficient to permit a comparable analysis. However, rough estimates of overall FLAR search and system effectiveness were computed. Both the system effectiveness and the search effectiveness for the FLAR system were less than that for the SLAR system.


## INTRODUCTION

### Objective.

The primary source of iceberg surveillance information in the vicinity of the Limits of All Known Ice (LAKI) is the Commander, International Ice Patrol's Ice Reconnaissance Detachment (ICERECDET), deployed from St. John's, Newfoundland. The IIP ICERECDET presently uses a HC-130H aircraft equipped with a pair of Motorola AN/APS-135 Side Looking Airborne Radars (SLARs) (two antennas mounted in pods on either side of the fuselage, with common signal processing) and one nose-mounted Texas Instruments AN/APS-137(V) Forward Looking Airborne Radar (FLAR). Observation windows allow visual observation of icebergs when weather permits.

The purpose of these patrols is to obtain current information on the location and classification of icebergs in the vicinity of the LAKI and to identify icebergs in the area of interest that will likely drift and ultimately impact the designation of the LAKI. Detection and identification of icebergs farther "upstream," while of great value in the drift model, is not a primary purpose of the ICERECDET. The surveillance information obtained in proximity to the LAKI is critical to providing current information to mariners.

The objective of the surveillance activity is to detect and classify icebergs and provide that information to the IIP for modeling predicted positions of ice and to develop appropriate warnings for the mariner. The purpose of this paper is to review the elements of that detection/classification process and provide the means for estimating the effectiveness of the process.


Codes

d / or
Special

A-1

## SURVEILLANCE CHARACTERISTICS AND PARAMETERS

### Search Mission Planning and Coverage.

Multiple, essentially daily (with allowance for aircraft maintenance and crew rest) sorties are performed during a nominal nine-day mission (every two weeks) to St. John's. Each sortie follows a preplanned flight path, the surface track of which is determined by the senior ICERECDET representative on the mission. Fight path planning is manual, with computer (PC) tool assistance. Because of generally restricted visibility, the altitude of the flight path is procedurally constrained to be above the 6000 ft. lower boundary of controlled airspace, and is normally at or near this limit. The sorties of a single mission collectively supply coverage of a swath following the boundaries of the (model predicted) Limits of All Known Ice, and extending, in searched surface area, from about 25 nm beyond this line to as far inside the line as can be covered for the combined sorties while satisfying fuel constraints.

### Search Patterns and Probability of Detection.

Patrol planning is based on the characteristics of the AN/APS-135 SLAR which is the primary detection device. Patrols are conducted using a Papa Sierra parallel search pattern with a track spacing of 25 nm. The SLAR range scale is set at 27 nm so that the SLAR coverage is nearly 200%. The purpose of the 200% coverage is to try to ensure that small icebergs and growlers are detected and to provide a means of determining target movement and aid in identification of a radar target as an iceberg. A representative search pattern is illustrated in Figure 1. Where possible, tracks are oriented in a N-S or E-W direction (or at least cardinal headings) to facilitate georegistration of the sightings which is accomplished manually on the gridded dry film processed by the SLAR. Most search patterns are less regular in practice because of the need to cover particular areas of the LAKI. The purpose of this paper is to estimate the overall effectiveness for a representative search as well as for any modification of that search.

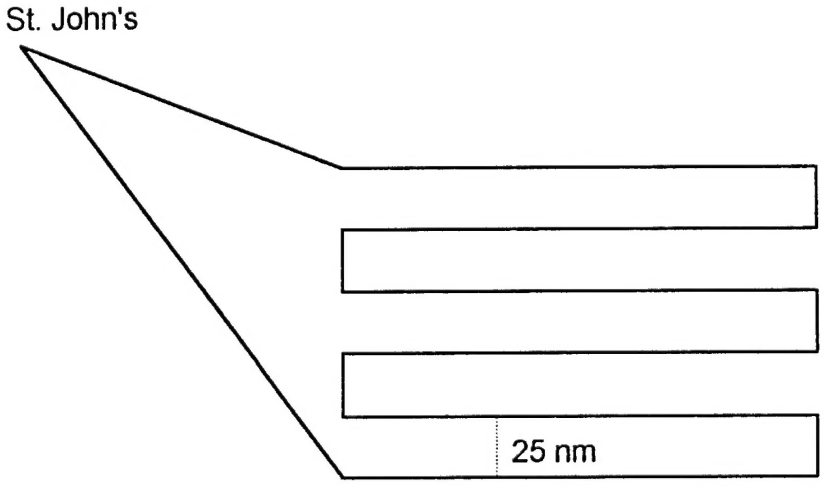


Figure 1. Representative search pattern.

**Iceberg Detection and Classification.**

Iceberg detections for each type of radar depends on human pattern interpretation of the CRT display associated with the system. During each track search segment, the SLAR and FLAR radar controls and displays are each manned by a crew member experienced in the operation of the device. When the display of either radar (both SLARs are controlled from a single console) indicates a potential surface object, the responsible operator makes a decision as to the validity of the detection, its categorization as iceberg, ship, or radar target, and, for objects adjudged icebergs, the size category ( growler, small, medium, large, and very large) and iceberg type. The operator then manually enters this information into a log of detected objects. During this process, each operator normally communicates orally with the other, and may, particularly in the case of initial FLAR detection, alert the other operator as to the presence and location of detections. A further description of the use of the SLAR/FLAR combination for iceberg detection and classification is contained in Appendix I. Theoretical detection properties of the AN/APS-135 SLAR are included in Appendix II and theoretical detection properties of the AN/APS-137 FLAR are included in Appendix III.

**AN/APS-135 Probability of Iceberg Detection.**

Three studies pertaining to the AN/APS 135-SLAR are available: the BERGSEARCH'84 evaluation performed by CANPOLAR consultants for the Canadian government, in which several air surveillance radars were evaluated (Rossiter *et al.*, 1985), and two other studies by IIP personnel and the CG R&D Center (Robe *et al.*, 1985; Alfutis and Osmer, 1988).

The BERGSEARCH'84 study examined five imaging radars, including the AN/APS 135-SLAR (Rossiter *et al.*, 1985). Surface truth data was obtained from a dedicated surface vessel and aerial cameras flown at low altitude in a small commercial aircraft. A variety of wind, viewing angle, and wave height conditions were encountered over the six day period of observation. Detection results are included in Table 1.

The 1985 IIP SLAR study evaluated only the AN/APS-135 for detection capability of bergs and small boats (Robe *et al.*, 1985). Accurate truth data was collected by object size. For the conditions of current operation, in seas up to 2 meters, for alerted operators, the Medium Iceberg (75m) target detection probability was estimated at nearly one hundred percent, while Small Iceberg (20-40m) and Growler (3 m to 15 m) detection probability was nearly 95%. The results are included in Table 2. Note that these results are based on an alerted operator analysis--specifically, an analysis of the film on a post-flight examination. The data were obtained using a search pattern with 5 km or 10 km track spacing, providing detection opportunities at various lateral ranges.

Table 1. BERGSEARCH '84 AN/APS-135 SLAR Data
(Alerted Operators/25 km range scale setting)

| TARGET TYPE** | Sea height (m) | | | Search altitude (ft)* | |
|---|---|---|---|---|---|
| | <1.0 | 1.6-2.1 | 2.5-2.9 | 4000 | 8000 |
| Medium Icebergs (50 to 100 meters) | 23/24 (0.96) | | | | |
| Small Icebergs (20 to 50 meters) | 10/12 (0.83) | 15/16 (0.94) | 8/8 (1.00) | 4/4 (1.00) | 11/12 (0.92) |
| Bergy Bits (10 to 20 meters) | 10/12 (0.83) | 23/32 (0.72) | 24/36 (0.67) | 7/8 (0.88) | 16/24 (0.67) |
| Growlers (<10 meters) | 0/2 (0.00) | 4/32 (0.13) | 1/24 (0.04) | 1/8 (0.13) | 3/24 (0.13) |

* Sea height of 1.6-2.1 meters only
** WMO classification

Table 2. AN/APS-135 SLAR Ice Target Data
(Alerted Operator)

| TARGET TYPE | SEARCH ALTITUDE/RANGE SCALE SETTING | | |
|---|---|---|---|
| | 2500 ft/25 km | 4000 ft/25 km | 8000 ft/50 km |
| Medium Iceberg (75 meters) | 7/7 (1.00) Mean $H_S$=0.8m | 6/6 (1.00) Mean $H_S$=0.7m | 7/7 (1.00) Mean $H_S$=0.6m |
| Small Iceberg (20 to 40 meters) | 41/42 (0.98) Mean $H_S$=1.4m | 37/37 (1.00) Mean $H_S$=1.4m | 34/39 (0.87) Mean $H_S$=0.8m |
| Growlers (3 to 15 meters) | 20/21 (0.95) Mean $H_S$=0.7m | 46/47 (0.98) Mean $H_S$=0.7m | 10/11 (0.91) Mean $H_S$=0.9m |

A third study by Alfutis and Osmer (1988) compared the AN/APS-135 SLAR with the AN/APS-131 AIREYE SLAR in the HU-25B aircraft. All flights were evenly spaced at 4000, 6000, 8000 and 10,000 ft altitude and conducted using a 50 km range scale setting. AN/APS-135 SLAR detections/opportunities over all altitudes for the three sizes of icebergs observed are included in Table 3. The one missed detection for the small iceberg was in the 20-27 nm range.

Table 3. AN/APS-135 SLAR Ice Target Data (Alfutis and Osmer, 1988)

| TARGET TYPE | System Detections/ Opportunities (POD) | Operator Detections/ System Detections (POD) |
|---|---|---|
| Small icebergs | 47/48 (0.98) | 45/47 (0.96) |
| Medium icebergs | 132/132 (1.00) | 119/132 (0.90) |
| Large icebergs | 17/17 (1.00) | 16/17 (0.94) |

The results from the three studies are summarized in Table 4. The BERGSEARCH 84 data represent 1.6-2.1 m sea height. The Robe *et al.* data for small icebergs were at 0.9-1.8 m sea height while the growler detections were at less than 1 m sea height. The Alfutis and Osmer data (column 2 in Table 3) were at 1-2.7 m sea height.

The experiments have shown that the AN/APS-135 SLAR seems to perform equally well in the 0-25 km and the 0-50 km range scale settings. As a first approximation to empirically estimate the probability of detection, we combine the above results in Table

5. These estimates generally represent an alerted operator situation and were computed in a post-flight laboratory setting.

Table 4. AN/APS-135 SLAR Ice Target Data Summary.

| TARGET TYPE | BERGSEARCH 84 8000 ft/25 km | Robe et al. 1985 8000 ft/50 km | Alfutis and Osmer, 1988 4000-10,000 ft/50 km |
|---|---|---|---|
| Large Icebergs | | | 17/17 (1.00) |
| Medium Icebergs | | 7/7 (1.00) | 132/132 (1.00) |
| Small icebergs | 11/12 (0.92)* | 34/39 (0.87) | 47/48 (0.98) |
| Growlers | 19/48 (0.40)* ** | 10/11 (0.91) | |

*Slightly different classification by size
**Includes Bergy bits and Growlers

Table 5. AN/APS-135 SLAR Ice Target Estimated System POD.

| TARGET TYPE | Estimated System POD |
|---|---|
| Large Icebergs | 17/17 (1.00) |
| Medium Icebergs | 139/139 (1.00) |
| Small Icebergs | 92/99 (0.93) |
| Growlers | 29/59 (0.49) |

The results in Table 5 represent system capability parameters. Alfutis and Osmer (1988) also recorded the operator misses. The probability of operator detection of a system detected target is included in column 3 of Table 3. Because there are no observations for growlers, the probability of operator detection for growlers is estimated to be the same as that for small icebergs. It is likely that this estimate overestimates the probability of operator detection. Thus, the probability of an iceberg being detected by the system and the operator is estimated in column 2 of Table 6. Alfutis and Osmer (1988) also recorded the number of times that the operator misinterpreted an iceberg as a ship. The correct classification factor for small icebergs was 43/45 (0.96), for medium icebergs was 115/119 (0.97), and for large icebergs was 1.00. As with growler detection, we assume that the classification probability for growlers is the same as for small icebergs. Applying these factors yields a final estimated operator probability of detection of icebergs in column 3 of Table 6.

Table 6. AN/APS-135 SLAR Ice Target Operator Adjusted POD.

| TARGET TYPE | Adjusted POD | Operator adjusted POD |
|---|---|---|
| Large Icebergs | (17/17)*(16/17) (0.94) | (17/17)*(16/17)*(17/17) (0.94) |
| Medium Icebergs | (139/139)*(119/132) (0.90) | (139/139)*(119/132)*(115/119) (0.87) |
| Small Icebergs | (92/99)*(45/47) (0.89) | (92/99)*(45/47)*(43/45) (0.85) |
| Growlers | (29/59)*(45/47) (0.47) | (29/59)*(45/47)*(43/45) (0.45) |

All of the experiments have consistently indicated that the AN/APS-135 SLAR detects targets uniformly across the lateral range of 27 nm when operated on the 50 km scale. Thus, it is reasonable to use a definite range law to represent the lateral range

curve. However, at the normal 6000 ft search altitude, the radar has a blind spot extending 2 nm on either side of the tack line. Hence, the lateral range curve will be as depicted in Figure 2.

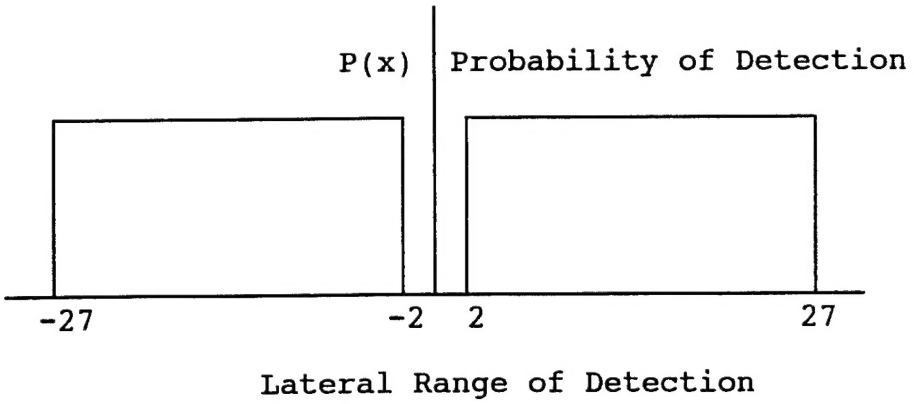


Figure 2. AN/APS-135 SLAR Estimated Lateral Range Curve.

The value of P(x) in Figure 2 will correspond to column 3 of Table 6 for each type of iceberg target.

**AN/APS-137 Probability of Iceberg Detection.**

Two evaluations (1991 and 1993) of the AN/APS-137 FLAR system have been conducted. However, the report of the second evaluation (Trivers and Murphy, in preparation) is not yet available for review. The 1991 AN/APS-137 FLAR evaluation (Ezman *et al.* 1993) involved HC-130 flights over a four day period and utilized altitudes and search ranges on either side of current FLAR operating conditions . Truth data was supplied by a surface vessel (USCGC BITTERSWEET). On each of the four days, one surveillance flight covering the entire area of interest was carried out by an AN/APS-135 SLAR equipped HC-130 for reference purposes. At the 32 nm range setting at a 6000 ft search altitude, the AN/APS-137 was found successful in four of four opportunities, and over four flights on the 64 nm scale, detected 17 of 18 icebergs. Over all flight altitudes and range settings (13 flights) the FLAR operators detected 48 out of 54 (POD = 0.89) actual iceberg targets, and correctly identified 39 of 48 (adjusted POD = 0.72) as icebergs. The data included in the report does not include the lateral range of detection. (It could be estimated from the target positions given in the report.) Enclosure 1 to the report suggests that a medium iceberg is detectable at the outer limits of the 8, 16, and 32 nm range scales. The 54 detection opportunities shown on the ground truth figures included 3 small, 44 medium, and 7 large icebergs. The report does not analyze detection by target type as was done in the SLAR analyses. Enclosure 2 to the report also notes that 2/3 of the screen was obscured with sea clutter when operating in the 32 nm scale. The report recommends operating on the 64 nm scale which has been adopted by IIP.

Data in the report are difficult to interpret. A cursory examination suggests that the probability of detection may actually be lower than that indicated above. The iceberg

searches in this analysis were conducted using the search mode. Parallel analyses of liferaft detection capabilities were conducted using periscope mode at lower altitudes. The 1993 analysis indicated that the best liferaft detection performance for FLAR was between 350° and 010°R and that performance dropped off significantly at relative bearings greater than ± 045°R. At ± 010°R, the lateral range on the 64 nm scale would be 11.1 nm; at ± 045°R, the lateral range on the 64 nm scale would be 42.3 nm. At this point, there is not enough information available to estimate whether the definite range law would apply, and if so, what is the appropriate lateral range at which detection will not occur?

The figures depicting the FLAR patrols and sightings indicate a significantly larger number of radar targets in the area than known icebergs and ships. It is suggested that a possible source of this discrepancy is the use of INS navigation and a repeat sighting on an adjacent search leg may also be identified as a separate target. Because of the nature of the ground truth, the above POD results should be used for medium icebergs.

**Probability of Classification.**

Given that the SLAR or FLAR system presents a radar target, it is important to the IIP to know whether the target is an iceberg or a ship. The SLAR operators have developed considerable expertise in recognizing icebergs. The correct classification factors in the Alfutis and Osmer (1988) study ranged from 0.96 to 1.00. These are probably upper bounds in that the various searches were conducted at 5 nm and 10 nm track spacing, giving the operators ample opportunity to acquire the target on subsequent passes and determine whether there is any movement in the target location. This is the principal mechanism for classifying the target as an iceberg. The Ezman *et al.* (1991) results for the FLAR operators yielded a correct classification factor of 0.81. It is recognized that the operators had no previous experience with using the FLAR to detect icebergs. Subsequent experience with the FLAR suggests that it is an excellent discriminator between ships and other radar targets (e.g., icebergs). Trivers and Murphy (1994) reported that the number of unidentified targets per flight was reduced from 3.6 in 1992 to 1.8 in 1993 after introduction of the FLAR.

The classification process using the SLAR and the FLAR are significantly different. For the SLAR, classification is made by determining that the target has relatively little movement (misclassifications of fishing vessels as icebergs are possible). During this process, except for operator attention, the detection process continues and images are presented on the dry film. With the FLAR, however, classification is accomplished in the imaging mode which requires a lock-on to the target. When this occurs, no detection is taking place. At a patrol speed of 250 kt, each minute spent imaging results in 4.2 nm of track not being searched. Using the FLAR as a sole detection device would severely limit its opportunity for imaging.

## SEARCH EFFECTIVENESS

### Basic Probability Model.

Current operation of the SLAR utilizes 200% coverage of a significant portion of the search region to minimize the probability of missing any icebergs in the area in the vicinity of the LAKI and to provide a mechanism for classifying targets as icebergs based on estimated movement. The following probability model can be used as a building block to estimate the overall probability of detection (effectiveness) for a given search area.

Let $A_i$ represent the $i$th area searched. Assume that any targets are randomly distributed in the area. Let $p_{ij}$ represent the conditional probability of detection of a target on the $j$th search of area $A_i$ given that the target is undetected prior to the $j$th search. Let $P_{ik}$ be the cumulative probability that the target is detected in area $A_i$ after $k$ searches of the area. Then

$$P_{ik} = p_{i1} + p_{i2}(1-p_{i1}) + \ldots + p_{ik}\prod_{j=1}^{k-1}(1-p_{ij}) \qquad (1)$$

Using the SLAR operator adjusted probabilities of detection in Table 6 and the similar data for the FLAR, application of equation (1) results in the search effectiveness shown in Table 7. This assumes that the values of $p_{ij}$ are equal for all searches.

Table 7. Search Effectiveness for SLAR Searches.

| TARGET TYPE | Probability of Detection after ith Search | | | |
|---|---|---|---|---|
| | 1st search | 2nd search | 3rd search | 4th search |
| Large iceberg | 0.94 | 0.9964 | 0.999784 | 0.999987 |
| Medium iceberg | 0.87 | 0.9831 | 0.997803 | 0.9997144 |
| Small iceberg | 0.85 | 0.9775 | 0.996625 | 0.9994938 |
| Growlers | 0.45 | 0.6975 | 0.833625 | 0.9084938 |
| FLAR | 0.72 | 0.9216 | 0.978048 | 0.9938534 |

### Search Effectiveness for ICERECDET Patrols.

ICERECDET patrols are typically conducted to cover a 90 nm wide swath along the entire LAKI. This usually requires four flight days to accomplish. When weather and the length of the LAKI permit, a fifth flight day is used to provide additional surveillance of the interior of the LAKI. With a 25 nm track spacing and the SLAR set on the 27 nm range scale (the lateral range curve in Figure 2 applies), the average search effectiveness is computed by weighting the POD in each section searched by the proportion of the area covered.

Consider the east-west legs of a regular four-leg parallel search indicated in Figure 3. The first outbound leg (assume the southernmost) will result in an area extending from 2 nm to 27 nm south to be covered at 100%. The 4 nm swath on the trackline will not be

covered on the first leg, but will be covered at 100% by the coverage on the second leg. Note that the region above the first leg is covered a second time. It is easy to show that all remaining areas except for the 4 nm swath along the track and a 27 nm swath above the last leg will be covered 200% (a second search with the same POD). The basic geometry is illustrated in Figure 3.

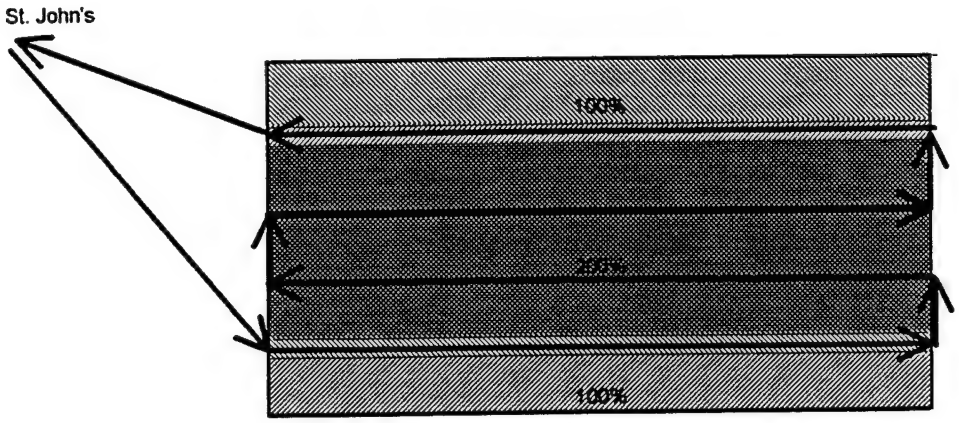


Figure 3. Search coverage.

Assume that there is no navigational error and that a regular (search legs of equal length) papa sierra parallel search is conducted with $n > 2$ search legs. For this model, we ignore the area covered on the turn legs. For a given target type, let $P_{11}$ be the probability of detection of the area searched at 100% and let $P_{22}$ be the probability of detection of the area searched at 200%. Then, for a 27 nm track spacing, it is easily shown that the effectiveness is computed as

$$E = (58P_{11} + (25n - 29)P_{22}) / (25n + 29). \tag{2}$$

The search effectiveness for a four leg and a six leg parallel sweep search pattern is included in Table 8 for each type of target.

Table 8. Search Area Effectiveness for SLAR Searches.

| TARGET TYPE | 4 leg search | 6 leg search |
|---|---|---|
| Large iceberg | 0.97 | 0.98 |
| Medium iceberg | 0.93 | 0.95 |
| Small iceberg | 0.92 | 0.94 |
| Growlers | 0.59 | 0.62 |

Using previous notation, the general formula for effectiveness is

$$E = (\sum_{i=1}^{n}\sum_{j=1}^{k}(P_{ij}A_i)) / \sum_{i=1}^{n} A_i \tag{3}$$

In applying equation (3), one must carefully lay out the search track and identify the coverage for each distinct area. The value of $P_{ik}$ is computed using equation (1).

The results in Table 8 represent the search effectiveness using SLAR with operators who will miss some targets and misclassify ones that they do detect assuming no navigational error in conducting the search. Because of the latter assumption, these are optimistic estimates. If operator nuances could be eliminated, we could compute the actual system effectiveness using the POD values in Table 5 in equation (2). The results, optimistic because of the assumed zero navigational error, are shown in Table 9.

Table 9. System Effectiveness for SLAR Searches.

| TARGET TYPE | 4 leg search | 6 leg search |
|---|---|---|
| Large iceberg | 1.00 | 1.00 |
| Medium iceberg | 1.00 | 1.00 |
| Small iceberg | 0.97 | 0.97 |
| Growlers | 0.63 | 0.66 |

It is expected that the digital upgrade to the AN/APS-135 SLAR along with the use of GPS will improve the georegistration, thereby assisting the classification process, and will permit digital enhancing to assist the operator in identifying targets. It is expected that the upgrade will permit the system to operate at the effectiveness shown in Table 9. It is possible that system effectiveness could be improved by means of digital enhancement.

For illustrative purposes, gross effectiveness results are computed for FLAR system and FLAR operator conditions. These are highly aggregated results and at best are crude estimates pending the development of a stronger data base. Based on Ezman *et al.* (1993), the average System POD for the FLAR is 0.89 and the Operator Adjusted POD is 0.72 for medium icebergs. Assuming that the definite range law holds over the 27 nm track spacing, equation (2) can be used to estimate the system and operator adjusted search effectiveness. The effectiveness results for four leg and six leg searches assuming no navigational error during the search are included in Table 10.

Table 10. Gross Effectiveness Estimates for FLAR Searches for Medium Icebergs.

| POD Basis | 4 leg search | 6 leg search |
|---|---|---|
| FLAR System | 0.94 | 0.96 |
| FLAR Operator | 0.83 | 0.86 |

The primary use of the FLAR has been to aid in the classification of radar targets. Although it has detected medium icebergs reasonably well, the FLAR also presented a significant number of unresolved targets during the evaluation. The performance of the FLAR with respect to small icebergs and growlers is unknown.

## SUMMARY AND CONCLUSIONS.

The several studies of the performance of the AN/APS-135 SLAR system have provided empirical data on which estimates of the probability of detection of various ice targets can be based. Using those results, estimates of the probability of detection, adjusted for operator misinterpretations and misclassifications, were computed and used in a model to estimate search effectiveness and system effectiveness for ice target types. The available study on the AN/APS-137 FLAR system was insufficient to permit a comparable analysis. However, rough estimates of overall search and system effectiveness were computed. Both the system effectiveness and the search effectiveness for the FLAR system were less than that for the SLAR system.

The overall system effectiveness and the operator adjusted effectiveness using the SLAR are generally very good, particularly for the larger icebergs under current operating conditions. Performance degrades significantly for growlers. FLAR performance lags behind SLAR for iceberg detection.

## REFERENCES


Alfultis, M. A. and S. R. Osmer, 1988, "International Ice Patrol's Side-Looking Airborne Radar Experiment (SLAREX) 1988," Appendix E in *Report of the International Ice Patrol in the North Atlantic*, Bulletin No. 74, 1988 Season, CG-188-43, Washington, DC.

Ezman, A. T., D. L. Murphy, V. L Fogt, and S. D. Reed, 1993, *1991 Forward-Looking Airborne Radar (FLAR) Evaluation*, International Ice Patrol Technical Report 93-01, Groton, CT..

Fung, Adrian K., 1994, *Microwave Scattering and Emission Models and Their Applications*, Artech House, Boston.

Masuko *et al.*, 1986, "Airborne Measurements of Microwave Scattering," *Journal of Geophysics Research*, Vol. 86, No. 11.

Robe, R. Q., N. C. Edwards, Jr., D. L. Murphy, N. Thayer, G. L. Hover, and M. E. Kop, 1985, *Evaluation of Surface Craft and Ice Target Detection Performance by the AN/APS-135 Side-Looking Airborne Radar (SLAR)*, Report No. CG-D-2-86, USCG Research and Development Center, Groton, CT.

Rossiter, J. R., L. D. Aresenault, E. V. Guy, D. J. Lapp, and E. Wedler, 1985, *BERGSEARCH'84: Assessment of Airborne Imaging Radars for the Detection of Icebergs*, Environmental Studies Revolution Funds Project, CANPOLAR Consultants, Ltd., Toronto, Ontario.

Skolnik, R. L., 1990, *Radar Handbook*, McGraw-Hill, New York.

Sittrop, H. 1977, "On the Sea-Clutter Dependency on Windspeed," *IEEE Proceedings, RADAR'77*, pp. 110-114.

Trivers, G. A. and D. L. Murphy, in preparation, *1993 Forward-Looking Airborne Radar Evaluation*, International Ice Patrol Technical Report 94-01.

Trivers, G. A. and D. L. Murphy, 1994, "Using Forward-Looking Airborne Radar in the International Ice Patrol Mission," International Ice Patrol paper.

# Appendix I. SLAR/FLAR Operational Modes

Detection and categorization for each type of radar depends on human pattern interpretation of the CRT display associated with the system. During each track search segment, the SLAR and FLAR radar controls and displays are each manned by a crew member experienced in the operation of the device. When the display of either radar (both SLARs are controlled from a single console) indicates a potential surface object, the responsible operator makes a decision as to the validity of the detection, its categorization as iceberg, ship, or radar target, and, for objects adjudged icebergs, the size category ( growler, small, medium, large, and very large) and iceberg type. The operator then manually enters this information into a log of detected objects. During this process, each operator normally communicates orally with the other, and may, particularly in the case of initial FLAR detection, alert the other operator as to the presence and location of detections.

FLAR lock-on requires operator placement of a cursor on the search display, which is variably illuminated by the sea clutter returns. A separate small CRT is used to present a pre lock-on range profile which is bracketed by parallel horizontal bars. The SLARs are consistently operated in the 27 nm full scale mode (1/500000 scale factor), and at the maximum PRF. Right and left side SLAR images (two film strips, 4.5 inches wide, developed in real time from CRT outputs, with dot density proportional to the log of the imaged dBms) take the form of small (.5 mm by 2 mm or more, depending on range) lozenge or lens-shaped dark regions elongated parallel to the aircraft motion, reflective of the limiting .47 degree azimuthal resolution of the SLAR. Image details pointed out by operators as a basis for categorization of an image as a ship included, on a SLAR image, an image extension significantly thinner than the main image, associated by the operator with a ship-borne radar antenna mounted aft of the ship. The central one-half of SLAR images on one or both sides are frequently uniformly gray to dark gray due to Bragg scattering from the sea surface. The outer half of SLAR images typically exhibits alternate bands of sea clutter and radar shadows on the sea surface. In some cases, one side of the film will be almost uniformly dark gray while the other side is almost totally unexposed due to a surface clutter viewing angle sensitivity. SLAR operators make adjustments to both antenna azimuth boresight and image saturation at their discretion.

FLAR inverse synthetic aperture (ISAR) images, when obtainable, are extremely unstable in the crossrange direction, taking the form of undulating bands (period of 4-8 seconds) of light and dark spots. Operator discrimination of a ship target was, in one case, based on the identification of a familiar (to the operator) pattern characteristic of a conning tower.

Each radar has aircraft motion compensation subsystems, and an independent navigation system. The AN/APS-137 FLAR provides a latitude/longitude and velocity readout on the auxiliary display for any cursor-selected object in track, while the AN/APS-135 SLARs provide for film display of latitude and longitude lines, from which object coordinates are estimated manually. Navigation errors are not insignificant (a nominal 5

nm is assumed for recorded positions), and may create erroneous correlations in a target-rich detection environment. Object resightings on subsequent flight path legs do not form the basis for additional operator log entries if correlation is considered adequate, but may result in reclassification or sizing of the object. Log entries are in pencil, and the latest sighting coordinates/time on a correlatable resighting is substituted as the sole log entry for the object. Subsequent to completion of the mission, the IIP senior officer reviews the logs of the radar operators, may supply additional changes or corrections, and merges the logs to create a unified list of sighting coordinates, times, and object category and size.

## Appendix II. Theoretical Detection/Classification Performance of the AN/APS 135-SLAR.

*System characteristics.* The AN/APS-135 SLAR is an X-band radar that scans the sea surface in a direction normal to the aircraft flight path. The radar image is displayed on a CRT as well as displayed and recorded on 23 cm dry process negative film. System parameters are included in Table II-1.

**Table II-1:** AN/APS 135 SLAR System Parameters

| | |
|---|---|
| Peak Power | 200 kW |
| Carrier Frequency | 9.250 (± .40) GHz |
| Pulse Width | .2 (± .02) μs |
| Pulse Repetition Frequency (PRF) | 375 or 750 (1/sec) |
| Antenna Azimuthal Half-Power Beamwidth | 0.47 (degrees, one-way) |
| Antenna Shaped Coverage in Elevation | -1.5 to -45 (degrees) |
| Peak Gain | 38.3 (including radome loss) |
| Depression Angle of Beam Peak | 1.5 (degrees) |
| Polarization | VV |
| CRT Spot Size | 1.15 mils ( to 1.80 mils) |
| Film Resolution | 20 lines per mm |

*Detection.* At the currently utilized 2 to 27 nm ground range half-swath, AN/APS-135 theoretical search performance is dominated by clutter rejection capability. At the 1/2 degree beamwidth, the SLAR is, at the minimum (2.24 nm) range, illuminating a 34m wide by 30m ($1020m^2$) long patch, which, from the Fung (1994) model, for 13 knot winds yields a backscatter coefficient of -28 dB $m^2/m^2$ at 63.5 degrees upwind for a cross section of $3.2m^2$. It would thus be necessary for a berg to have an area, viewed from above at 63.5° of about $63m^2$ to achieve a single-pulse signal to clutter ratio of 1. This, fortunately, is not necessary for two reasons:

(1) Since the aircraft is moving, substantial clutter decorrelation is obtained because of the differential Doppler across the clutter patch. A d meter aircraft forward motion produces a change $\Delta R = xd/R$ in a clutter patch that is originally at distance R perpendicular to the track and x downtrack from the original aircraft position. For d = 25 m, the screen displacement is equal to the film resolution of .05 mm. The system must effectively be integrating over the (approximately 140, at 250 knots) pulses received during this motion. For a scatterer at the trailing outer edge of the illuminated patch (assumed temporarily to be the 3 dB beamwidth) the ΔR during the 25 meter motion is about .20 meters, or more than six complete wavelengths, so that the round trip phase shift is about 25 π radians, or 12.5 cycles. This corresponds to a Doppler spectrum spread (front to back of beamwidth) of $\Delta f_D$ = 134 cyc/sec (independent of range). From Skolnik (1990), the implied correlation time is $T_i = 0.65/\Delta f_D = 0.0049$ sec and the equivalent number of independent samples is the total integration time, 0.1866 sec (at 250 knots),

divided by $T_i$, or 38 samples. If the pulses were coherently integrated, a substantial deduction in clutter power would take place. For incoherent integration, the variance of the clutter image from screen point to screen point is greatly reduced (accounting for the uniform gray appearance of the screen), and the return is very nearly proportional to the previously computed patch cross section, for each pulse. This accounts for the uniform gray, rather than speckled, appearance of the screen clutter. Targets are, in general, substantially smaller than a beamwidth in extent, and thus are consistent with perhaps a few independent samples; the radar cross section behavior is, however, somewhere between Swerling 1 and Swerling zero (nearly constant for short times) because of the volume scatterers. The region of screen spots characterizing the target image as a whole should thus, approximately, reflect the sum of the radar cross sections of the clutter and target, with some intensity variation near the image center, where the small target phase center to clutter phase center displacement provides the least phase shift change during spot integration.

(2) The visual detection mechanism provides sub-clutter visibility. A berg of only 12.7m$^2$ actual presented area, as viewed from above, will produce a twenty percent (+2 dB) change at minimum range, relative to the background clutter return, as computed above. If the dynamic range of the log-proportional photographic image is only 20 dB, a ten percent increase in image exposed dot density (for the negative image) occurs. This may well be visible and recognizable to the trained operator, provided the image is well scrutinized. Since an alerted operator cannot be guaranteed in the operational case, this condition represents a theoretical maximum.

As groundrange increases slightly, the sea clutter coefficient drops slightly faster than the ice backscattering coefficients (for the top ice surface). Fung (1994) yields a top surface coefficient decline of -4 dB at 70°, corresponding to a slant range of 2.91; Masuko *et al.* (1986) predicts a decline of -3 dB to -31 dB for X-band, HH sea clutter at this incidence angle. Since the clutter patch width increases by about 30% (1 dB), a 2 dB drop in clutter is anticipated. (The subjective appearance of the screen suggests no change, however.) The drop in ice top surface backscatter coefficient may be partly compensated by increased contribution from the side. Thus, something between less than a 1 dB (30%) increase in berg area is needed to preserve the ten percent intensity margin.

From 70° to 85° incidence, Skolnik (1990) suggests a decline of about 3 dB in backscattering coefficient for "medium" seas (about 15 knots; the comment in Skolnik (1990) is, however, " the variability of sea echo data is great, and does not warrant the precision with which Figure 3 is drawn"). At 85°, the range of 11.5 nm produces an increase in clutter patch length sufficient for a 6 dB increase, so that an increase in clutter cross section of 3 dB is anticipated. In the same interval, the top surface backscattering coefficient declines by 18 dB, so that an increase of 21 dB, to about 1600 m$^2$, would be necessary to achieve the required intensity margin based on top surface alone. This is consistent with detection of very large tabular growlers only. A presented side area of about 40m$^2$ near normal or about 60m$^2$ at a mean incidence angle of 45° is, however,

sufficient to meet the detection requirement. That some growlers and small bergs may not produce an adequate side + top cross section to be detected is apparent.

Beyond about 85°, the backscatter coefficient theoretically (Skolnik, 1990) drops rapidly enough to compensate for the length increase. At the 27 nm range, the clutter patch is 386 m wide by 30 m long (11580 $m^2$) and the angle of incidence relative to the sea surface is 87.9°, so that the sea backscatter coefficient is down by (very approximately) -40 dB for the upwind, 20 knot case. This condition creates a very small backscattering coefficient for the ice top surface as well, but berg sides may be well imaged. The observed image on the SLAR display implies that the clutter cross section is, in very large (hundreds of meters) patches, much brighter than the estimated -40 dB coefficient would imply. These alternate with light regions of approximately the same size, which are white on the negative, may be radar shadows large enough to partially obscure growlers. The dark (high clutter) SLAR patches are approximately as dark or darker than the 85° incidence region. At the reduced top surface ice cross section expected for this range (-35 dB or less), growlers and bergs will only be visible in the anomalous, high clutter regions if the unsubmerged (and visible, submerged) presented cross section (in the colloquial sense) approaches 100 $m^2$. In regions of apparent low clutter at maximum range, side aspect areas as small as 5-10 $m^2$ are probably detectable.

At higher wind velocity (about 30 knots), Masuko *et al.* (1986) suggests about a +5 dB increase in backscatter coefficient near the inner search boundary, which yields a 37 $m^2$ top aspect area, or about 20 $m^2$ side area for detection, by the previous criterion. Data beyond 70° incidence for this velocity suggests a less rapid decline (only about 1 dB to 85 °), so that an equivalent side area of nearly 100 $m^2$ is necessary for detection at 12 nm range. Requirements beyond this range are uncertain. The above computations for upwind SLAR performance are improvable by about 5 dB for crosswind conditions.

*Imaging.* SLAR imaging is compromised principally by the 0.47 degree (power, one-way) azimuth beamwidth. The form of images, and hence the ability of the AN/APS-135 SLAR to distinguish icebergs from ships, depends not only on this parameter, but on the threshold and saturation dBsm values. A principle means of distinguishing ships is the achievement of saturation dot density over a single, .06 mm width corresponding to the 30 meter single-pulse return. It is possible that this effect may not be observed if the threshold has been set too low, permitting bergs to also achieve saturation rapidly. The robustness of imaging guidelines within operator-permitted panel adjustments may warrant brief investigation.

[ BLANK ]

## Appendix III. Theoretical Detection/Classification Performance of the AN/APS-137 FLAR.

*System characteristics.* The AN/APS-137 FLAR is a state of the art X-band marine surveillance radar developed by Texas Instruments. It operates in either a search mode (real aperture) or an imaging mode (inverse synthetic aperture, ISAR). There are three variations of search: search mode (wide-area searches), navigate mode (wide-area search with low antenna scan rate), and periscope mode (short range, low altitude, for small targets). The operating parameters are summarized in Table III-1.

**Table III-1:** AN/APS 137 FLAR System Parameters

| Search Mode | Range Scales (nm) | Peak Power (kW) | Scan Rate (RPM) | Pulse Width(sec) /PRF | Beam Width (deg) Az/Elev | Carrier Frequency (GHz) | Wave form |
|---|---|---|---|---|---|---|---|
| Periscope | 8,16,32 | 500 | 300 | .5μs/2000 | 2.4/4 | 9.05-10.55 | LFM |
| Search | 8,16,32,64, 128,200 | 500 | 60 | .5μs/400 | 2.4/4 | 9.6-9.7 | LFM |
| Navigate | 1-200 | 500 | 6 | .5μs/400 | 2.4/4 | Variable | PRN |
| Image | N/A | 500 | N/A | .5μs/mode | 2.4/4 | 9.6-9.7 | LFM |

LFM = Linear Frequency Modulation (Chirp)
PRN = Pseudo Random Noise

*Search modes.* The AN/APS-137 FLAR employs traveling wave tubes (TWT) for high peak power and high resolution waveforms. The 9.05 - 10.55 GHz swept band for the chirped pulse provides a range resolution of about 0.10 meters, and approximately 16 pulses are integrated per scan (scan to scan integration may also be performed). The high resolution waveform produces substantial reduction in single pulse clutter cross section variance, since scatterer returns for the frequencies of the chirped pulse are integrated. With a vertical beamwidth of only 4 degrees, the system is designed to view both sea and targets at near-grazing incidence angles. The 2.4 degree azimuth beamwidth is illuminating a large patch of sea water; at, for example, 30 km, a swatch 1254 m by 0.10 m, for an illuminated area of 125.4 $m^2$. The nominal mean backscattering coefficient is, however, no larger than about $10^{-3.5}$ at X-band (Sittrop, 1977), and may be much smaller, so that the clutter mean cross section per illuminated range bin is only about 0.04 $m^2$. The principal clutter rejection device is thus low incidence angle.

Under these conditions, it is known that the clutter spectrum is better characterized by a Weibull or log-normal distribution, so that single pulses may provide spikes well above the mean clutter cross section. The standard procedure for a high range resolution radar is to set the single bin detection threshold to provide an adequately low false alarm rate over the all the range bins, which determines the single-bin S/C for detection, and the consequent theoretical probability of detection performance for the system. Such a computation is appropriate where the theoretical clutter backscattering coefficient is

reliably known from measurement, preferably supported by theoretical predictions. This is, however, not the case in the region of FLAR (or, for the most part, SLAR) operation). Skolnik (1990) (Chapter 26) cites experimental errors as great as 10 dB for measurements of this parameter. Although recent theoretical advances are obtaining good agreement with measured coefficients in the 0-60° incidence angle range, extension to higher incidence angles has not proven possible. For example, Fung (1994) does not include updated versions (or even the original versions of his own earlier (1977)) results for backscattering at low incidence angle and simply omits this regime. The earlier results were used in the BERGSEARCH'84 (Rossiter *et al.*., 1985). There is, moreover, evidence from SLAR mapping of what may be long-period wavelength (100s of meters) swells that are producing radar shadows over large areas; these are probably hiding low-lying bergs and growlers from both SLAR and FLAR.

The disappointing performance of FLAR, relative to the SLAR, in detecting small bergs (which is suggested by the studies, and is experienced by ICERECDET personnel) is at first somewhat difficult to understand in the light of the advertised capability of the system, which, according to Jane's (1994), is Periscope mode detection (of periscopes) at up to 32 km range. Comparison of target characteristics alone is relevant to understanding the AN/APS-137 performance for ice targets, since clutter return is similar in size and spectrum for periscope and ice detection. However, periscopes are hard targets while ice and life rafts are not. The fact that the entire periscope will, in this mode, probably appear in one or two 10 cm range bins implies a cross section of about perhaps 0.10 $m^2$ or more in one bin.

Comparison with typical iceberg X-Band cross sections for narrow-band radars is essentially impossible, since an entire berg is rarely viewed in a single bin for this radar. An iceberg will have returns for each 10 cm bin from both surface and volume elements contained in that bin. A berg that presents as much as 2.5 $m^2$ (assuming -10 dB $m^2/m^2$ at or near normal incidence) of presented, near normal surface aspect in a single range bin, regardless of gross size, is thus required to provide a single pulse signal to clutter ratio equivalent to the periscope (which is, moreover, required to extend a greater distance above the mean ocean surface in heavy seas).

Fung (1994) presents backscattering coefficients for multi-year sea ice and is used as an approximation to estimate the effects for glacial ice, which is known to have different radar reflectivity. Those coefficients show that the decline in cross section with angle of incidence approximates a cosine dependence until about 60°, but is steeper thereafter, implying that the radar cross section drops off like the colloquial cross section of the berg normal to the sightline out to about 60°, implying a strong contribution from bubble scatterers. Range bin cross sections subsequent to the first few will be larger in normal colloquial cross section area, but will have interior (bubble) scatterers partly due to greatly attenuation by absorption and scattering, depending on the depth, and are thus more dependent on surface scattering to achieve return. Medium to large bergs will nevertheless frequently present sufficient surface area at reduced aspect angles to exceed the required threshold. Considerations are similar in the Search mode, for which each

downrange cell is about 0.75 meters, and the number of pulses integrated per scan is also 16. The single pulse S/C will not be as good for this mode, but target cross section variability will be reduced, perhaps explaining the subjective lack of difference in performance in these modes as observed by operators.

*Possible sources of FLAR performance improvement.* Ocean backscattering cross section variation with aspect angle and wind direction may be adequately compensated in the system design for metal targets, but flight path planning to minimize this parameter could be used to achieve increased performance for low cross section iceberg targets for the AN/APS-137. The maximum achievable improvement for one meter seas at 20 knots is about six dB (Fung model results with the crosswind direction providing minimum backscatter; downwind and upwind results are similar (Fung, 1994)).

Although clutter samples are substantially decorrelated by the high resolution waveform, additional decorrelation is probably achieved at side aspects (which would yield 8 decorrelated samples at the side aspect even without the high resolution waveform, because of the Doppler spread from front to back of the clutter patch. Each FLAR pulse is, in fact producing a clutter sample of reduced cross section variance because of the chirped waveform, but the side aspect can additionally improve pulse to pulse decorrelation.) This implies that potential targets not detected from a front aspect should be reexamined if possible at the $\pm 90°$ aspect.

FLAR operation in the Navigate mode should provide superior clutter rejection at the expense of 6 rpm search. Although the number of samples is the same for each mode, the Navigate mode frequency diversity provides more complete clutter decorrelation.

It is possible that the unique dynamic characteristics of iceberg motion arising from relatively small separation of the center of mass and center of buoyancy can be exploited to improve/stabilize iceberg images only on the FLAR display. A shortcoming of this approach is that the small fraction of bergs with very high bubble density may not exhibit the anticipated dynamic characteristics.

*Imaging mode.* Imaging mode results are disappointing for the FLAR, as described above. Severe distortion is producing images in the form of undulating bands of pixels of various brightness for both bergs and ships. The advertised performance for this imaging mode is adequate to perform ship typing and assess battle damage (Jane's, 1994). The performance being achieved in the current operational mode is clearly not this good for bergs or ships, suggesting a possible mismatch of operating conditions to system design. The system must effectively establish the parameters of a matched filter, measuring and subtracting the unwanted frequency components to make ISAR work (Skolnik, 1990). The current image is suggestive of a raw ISAR image, in which the crossrange cell to Doppler frequency assignment does not vary periodically with the observed target rotation frequency to produce a stable image. Discussions with Coast Guard personnel at Coast Guard Air Station Elizabeth City, NC indicate that this type of image is, in fact, routinely observed, and that the Jane's description of the images in the

fleet imaging mode is not standard. It is claimed that image classification by an experienced operator is a high confidence event, but that operator skill and knowledge of the system are essential to achieve the current high level of performance. Note that time spent in the imaging mode takes away from detection opportunity time. When the FLAR is in the imaging mode, it will lock-on to the target. When this occurs, no detection is taking place. At a patrol speed of 250 kt, each minute spent imaging results in 4.2 nm of track not being searched. Using the FLAR as a sole detection device would severely limit its opportunity for imaging.